

# Delaying visually guided saccades by microstimulation of macaque V1: spatial properties of delay fields

Edward J. Tehovnik, Warren M. Slocum and Peter H. Schiller

Department of Brain and Cognitive Sciences, Massachusetts Institute of Technology, E25-634, Cambridge, MA 02139, USA

**Keywords:** current spread, electrical stimulation, occipital cortex, phosphenes, rhesus monkeys

## Abstract

Electrical microstimulation of macaque primary visual cortex (area V1) is known to delay the execution of saccadic eye movements made to a punctate visual target placed into the receptive field of the stimulated neurons. We examined the spatial extent of this delay effect, which we call a delay field, by placing a  $0.2^\circ$  visual target at various locations relative to the receptive field of the stimulated neurons and by stimulating different sites within the operculum of V1. A 100-ms train of stimulation consisting of current pulses at or less than  $100 \mu\text{A}$  was delivered immediately before monkeys generated a saccadic eye movement to the visual target. The region of tissue activated was within 0.5 mm from the electrode tip. The depth of stimulation for a given site ranged from 0.9 to 2.0 mm below the cortical surface. The location of the receptive fields of the stimulated neurons ranged from  $1.8$  to  $4.4^\circ$  of eccentricity from the center of gaze. Within this range, the size of the delay field increased from  $0.1$  to  $0.55^\circ$  of visual angle. The shape of the field was roughly circular. The size of the delay field increased as the stimulation site was located further from the foveal representation of V1. These results are consistent with the finding that phosphenes evoked by electrical stimulation of human V1 are circular and increase in size as the stimulating electrode is placed more distant from the foveal representation of V1.

## Introduction

Electrical microstimulation of primary visual cortex (area V1) interferes with the execution of visually guided ocular responses (Schiller & Tehovnik, 2001; Tehovnik *et al.*, 2002, 2004; Tehovnik & Slocum, 2003, 2005; Slocum & Tehovnik, 2004; for a review see Tehovnik *et al.*, 2005). Previously, we have shown that microstimulating V1 while a monkey is fixating a spot of light delays the execution of a visually guided saccadic eye movement to a target placed into the receptive field of the stimulated neurons (Tehovnik *et al.*, 2004). We believe that this delay effect is caused by disruption of the normal processing of visual information by the V1 neurons (Tehovnik *et al.*, 2004; Tehovnik & Slocum, 2005), and this effect is possibly related to the masking of visual targets induced by transcranial magnetic stimulation of human V1 (Kammer *et al.*, 2005). Neurons involved in the delay effect exhibit excitability properties that are similar to those of the neurons in V1 of humans, which when stimulated elicit a phosphene (Brindley & Lewin, 1968; Dobelle & Mladejovsky, 1974; Rushton & Brindley, 1978; Tehovnik *et al.*, 2004). Therefore, it is plausible to assume that a phosphene-like percept is evoked every time electrical stimulation is delivered to V1 of monkeys.

In this study, using the delay of visually guided saccades by electrical stimulation, we show that the size of the visual field affected by the stimulation varies according to the site of stimulation in V1. We call the field affected by the stimulation a delay field. We found that the further a stimulation site is from the foveal representation of V1 the larger the delay field. In addition, we found that delay fields are

roughly circular. We suggest that mapping out delay fields allows us to make inferences regarding the size and shape of phosphenes elicited from V1 of monkeys.

## Materials and methods

### Subjects

Three adult rhesus monkeys (*Macaca mulatta*), designated C, H and M, were used. Access to water was limited before each day of experimental testing. After testing, the monkeys were allowed to drink until sated before being returned to the vivarium. Monkeys were provided for in accordance with the National Institutes of Health Guide for the Care and Use of Laboratory Animals and with the Guidelines of the Massachusetts Institute of Technology Committee on Animal Care.

### Surgery

Monkeys were anesthetized intravenously with pentobarbital (20 mg/kg) and prepared for aseptic surgery. A scleral search coil was implanted (Judge *et al.*, 1980), and a stainless-steel post, used to restrain the head, was secured to the skull with titanium screws and acrylic cement. Subsequently, a recording chamber was fixed over the right V1.

### Behavioral tasks

The animals, with head fixed in position, faced a computer monitor (Sony Multiscan E210) positioned 57 cm away in a dimly lit room. An animal was trained first to fixate a central spot ( $0.1^\circ$  in diameter,

Correspondence: Dr E. J. Tehovnik, as above.

E-mail: tehovnik@mit.edu

Received 28 June 2005, revised 14 August 2005, accepted 22 September 2005

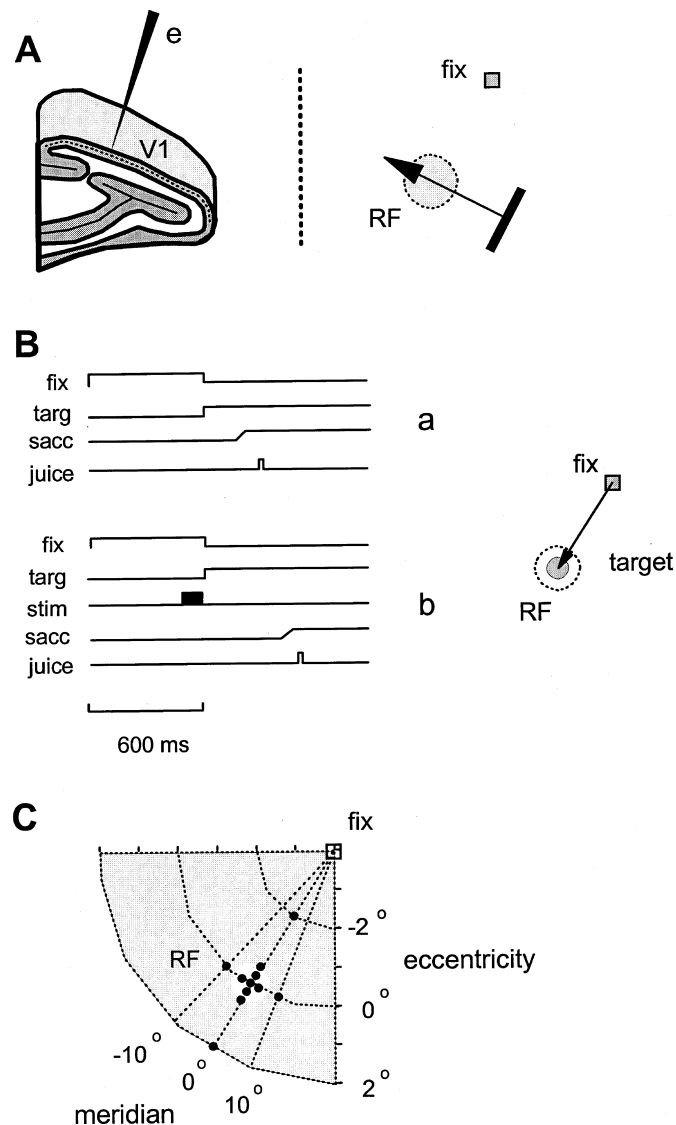


**FIG. 1.** Methods. (A, left) All electrodes (e) were lowered into V1 such that they penetrated V1 perpendicular to the cortical surface. (A, right) Receptive fields (RF) were mapped by moving a bar of light at different orientations across the visual field, as the monkey remained fixated (fix). (B) For all trials, an animal fixated a spot for 600 ms (fix) otherwise the trial was aborted and no juice reward was delivered. Two types of trials were interleaved to study the stimulation-evoked delay effect. (a) Following fixation, a target (targ) was presented in (or outside) the receptive field of the stimulated neurons following the extinction of the fixation spot (also see illustration to right). The animal was required to generate a saccade (sacc) to the target within 500 ms to obtain a juice reward (juice). (b) Following fixation, a target (targ) was presented in (or outside) the receptive field of the stimulated neurons following the extinction of the fixation spot. Before the end of the fixation period, a train of electrical stimulation (stim) was delivered to the neurons. The animal was required to generate a saccade (sacc) to the target within 500 ms to obtain a juice reward (juice). (C) The target was presented at various locations with respect to the center of the receptive field of the stimulated neurons. The target could occur from positive to negative  $10^\circ$  of meridian with respect to the center of the receptive field of the stimulated neurons and from positive to negative  $2^\circ$  of eccentricity with respect to the center of the receptive field. The target used was brighter than background at 33% contrast and was  $0.2^\circ$  in diameter. The fixation location (fix) of a monkey's center of gaze and the receptive-field location (RF) of the stimulated neurons is indicated.

153  $\text{cd}/\text{m}^2$ ) and to then make a saccadic eye movement to a visual target ( $0.2^\circ$  in diameter, 153  $\text{cd}/\text{m}^2$ ) that appeared at various locations on the monitor screen (with background luminance that could range

from 7.7 to 76.7  $\text{cd}/\text{m}^2$ ). This task had two forms. In the first, the fixation spot remained on for 2–4 s and the animal had to maintain fixation until the spot was terminated and a target appeared. While the animal maintained fixation, a bar (153  $\text{cd}/\text{m}^2$ ) was swept across a restricted region of the monitor screen to map the receptive field of the neurons recorded from V1. After each sweep, the target appeared and the animal was rewarded with a drop of apple juice after a saccade had been made to the target. The orientation and size of the bar, as well as its direction of motion, were varied systematically until the location of the receptive field was determined (Fig. 1A, right).

For the second task, animals were required to fixate a spot of light ( $0.1^\circ$  in diameter, 153  $\text{cd}/\text{m}^2$ ) for 600 ms, after which a visual target ( $0.2^\circ$  in diameter, 153  $\text{cd}/\text{m}^2$ ) was presented in one of several locations for 500 ms (Fig. 1C). Some of these locations were in the receptive field of the neurons under study. The background luminance of the monitor was fixed at 76.7  $\text{cd}/\text{m}^2$ . Monkeys received a juice reward for generating a saccade to the target within 500 ms following target onset (Fig. 1B, a). During fixation, an animal was required to keep its eyes within a  $0.5 \times 0.5^\circ$  window; otherwise the trial was aborted. During experimental sessions a 100-ms train of electrical stimulation was delivered to V1 on 50% of trials in a random order (Fig. 1B, b). The train commenced 100 ms before the end of the fixation period. The latency with which saccades were generated to the visual target constituted the primary data for the study.

Typically, 11 target positions were tested, one at the center of the receptive field, six along the axis of eccentricity and four along the arc of meridian (Fig. 1C). For stimulation sites nearer the foveal representation of V1 the target positions nearest to the receptive-field center were  $0.1^\circ$  off center, whereas for stimulation sites further from the foveal representation the target positions nearest to the receptive field center were  $0.2^\circ$  off center. This was done because we observed early in our investigation that the size of a delay field increased with increases in eccentricity of the receptive-field center of the stimulated neurons.

#### Estimating electrode depth

For all electrode penetrations made into V1 (Fig. 1A, left), a standard method was used to deduce the electrode depth with respect to the top of cortex (Tehovnik *et al.*, 2002, 2003). Once single units were encountered, their receptive field was mapped and the electrode was adjusted in depth until the unit activity was just detectable at the top of cortex. This point marked the initial depth at the top of V1. At the end of a test session the depth at the top of V1 was re-measured by noting the point at which unit activity to visual stimuli became barely detectable as the electrode was slowly withdrawn. The estimated depth at the top of V1 was taken as the average of the initial and final depth estimates.

#### Data collection and analysis

A PDP-11/73 computer controlled the presentation of visual stimuli, the delivery of electrical stimulation, the collection of multiple-unit spikes, the acquisition and display of eye position (sampled at 200 Hz), and the delivery of juice.

#### Electrical stimulation and collection of multiple-unit spikes

Electrodes were introduced perpendicular to the cortical surface with a hydraulic microdrive (Fig. 1A, left). Constant-current charge-balanced biphasic pulses were delivered to the brain via a monopolar glass-coated platinum-iridium electrode (at 0.3–0.5  $\text{M}\Omega$  tested at 1 kHz) using a Grass S88 stimulator attached to a pair of constant-current

stimulus isolation units (Grass PSIU6B, Quincy, MA, USA). For each biphasic pulse, an anodal and cathodal pulse followed in immediate succession to produce anode-first pulses. Both pulses of a pair had the same amplitude and duration. Current was measured by the voltage drop across a 1000- $\Omega$  resistor that was placed in series with the return lead of the stimulator. The current was monitored continuously using an oscilloscope and was read as the amplitude of one pulse (anodal or cathodal) of a biphasic pair. The stimulation parameters used were as follows: current was 50 or 100  $\mu$ A, and the pulse duration, pulse frequency and train duration were fixed at 0.2 ms, 200 Hz and 100 ms, respectively.

Multiple-unit recording was performed using the same electrode that had been used in the stimulation experiments to measure the responsiveness of cells to the presentation of a punctate visual target, i.e. the same target that had been used in the stimulation experiments. The action potentials were amplified (Bak A-1B, Germantown, MD, USA) and filtered (Krohn-Hite 3750, Horsham, PA, USA), isolated with a window discriminator (Bak DIS-1), and displayed on an oscilloscope (Tektronix TDS-210). At the start of unit recording the window discriminator was adjusted so that the units were barely detectable. The window settings were fixed while mapping the receptive-field location of the cells under study. The computer counted the number of multiple-unit spikes occurring over a 100-ms period following the onset of a bright circular 0.2° visual target illuminated at 33% contrast (Michaelson contrast). On control trials in which no target appeared the unit activity was sampled over the same 100-ms period.

## Results

### Stimulation sites

For monkey C, the penetrations yielded cells with receptive-field centers varying from 1.8 to 4.4° of eccentricity and from 209 to 246° of meridian; for monkey H, the penetrations contained cells with receptive-field centers varying from 2.6 to 3.9° of eccentricity and from 256 to 259° of meridian; and for monkey M, the penetrations had cells with receptive-field centers varying from 2.8 to 4.6° of eccentricity and from 225 to 250° of meridian. A total of 41 sites were analysed in detail: 37 sites from monkey C, three sites from monkey H and one site from monkey M.

### Location of the visual target

The location of the visual target with respect to the receptive-field center of the stimulated neurons had an effect on the latency of visually guided saccades during stimulation trials. As already noted, the background luminance of the monitor was set at 76.7 cd/m<sup>2</sup> and the 0.2° diameter target was set at 153 cd/m<sup>2</sup> (i.e. 33% contrast). Figure 2 illustrates data from one stimulation site containing units whose receptive-field centers were at 233° of meridian and at 4.3° from the fovea. The maximal increase in saccadic latency due to stimulation with a 100- $\mu$ A current was observed when the target was positioned at the center of the receptive field of the stimulated neurons (Fig. 2A and B). The magnitude of the latency increase dropped systematically as the distance between the target and receptive-field center was increased. For target eccentricities beyond 0.5° from the receptive-field center, the stimulation became ineffective (Fig. 2A). In addition, for target meridian values outside of the receptive-field of the stimulated neurons, the stimulation became ineffective (i.e. at 10° of meridian from the receptive-field center, which corresponds to 0.8° of visual angle from the receptive-field center) (Fig. 2B).

The latency difference for stimulation trials as compared with non-stimulation trials was computed for the 100- $\mu$ A current condition while target position was varied. The greatest latency difference was observed when the target was situated at the receptive-field center of the stimulated neurons, and the latency difference declined as the target was presented further away from the receptive-field center (Fig. 2C and D).

Finally, the multiple units at the stimulation site responded maximally when the same visual target as used in the stimulation experiment was flashed in the center of the receptive field (Fig. 2E and F). The magnitude of this response dropped as the target was placed further away from the center of the receptive field. The decline in the unit response was less rapid than the decline in latency for comparable distances from the receptive-field center (compare Fig. 2E and C; compare Fig. 2F and D).

### Size of the delay field

The portion of the visual field producing a delay in visually evoked saccades increased with increasing eccentricity of the stimulated V1 representation. Figure 3 shows how we defined the size of a delay field for any given site of stimulation. The maximal latency difference in saccadic eye-movement initiation occurred when the visual target was placed in the center of the receptive field of the stimulated neurons (Fig. 3A, zero eccentricity). As the target was placed at progressively more distant locations relative to the center of the receptive field, the magnitude of the saccadic delay decreased. The latency-difference data in Fig. 3A were normalized such that the maximum latency difference was set to one (Fig. 3B). The size of a delay field was measured by noting the negative and positive target-eccentricity values at 50% of peak latency difference [Fig. 3C; size = 0.33 – (–0.16)°]. The size of the delay field (*s*) in this case was 0.49° of visual angle.

As just discussed, the size of a delay field was characterized by the width of a delay-field curve at half of the maximal delay. The half amplitude points were ascertained by interpolating between the relevant pair of measurements on each side of the curve (Fig. 3C). Owing to the granularity of sampling, it was sometimes possible for one point of a pair to lie close to zero (i.e. within the noise). An example of this can be found on the right-hand side of the curve in Fig. 3C. In cases in which this occurred, the delay field size may be somewhat overestimated, as the curve may in fact reach zero closer to the center than indicated by sampling.

A population analysis based on 41 sites ascertained that the size of the delay field increased with increasing eccentricity of the stimulated V1 representation (Fig. 4A;  $r = 0.81$ ,  $n = 41$ ,  $P < 0.01$ ). The region stimulated in the operculum is expressed in Fig. 4A as receptive-field eccentricity, which denotes the location of the receptive field center of the stimulated neurons relative to the center of gaze defined by the location of the fixation spot. For these experiments a current of 100  $\mu$ A was used. For six sites, the size of the delay field using two current levels (i.e. 50 and 100  $\mu$ A) was compared. Using 50  $\mu$ A the average size of the delay field was 0.26° of visual angle; using 100  $\mu$ A the average size was 0.35° of visual angle. The size of the delay field using a 50- $\mu$ A current was a fraction (74%) of that found using a 100- $\mu$ A current. This difference is significant ( $t_5 = 3.8$ ,  $P < 0.02$ ).

### Shape of the delay field

The shape of a delay field was found to be roughly circular. Data are shown for two sites (Fig. 5) in which the size of the delay field

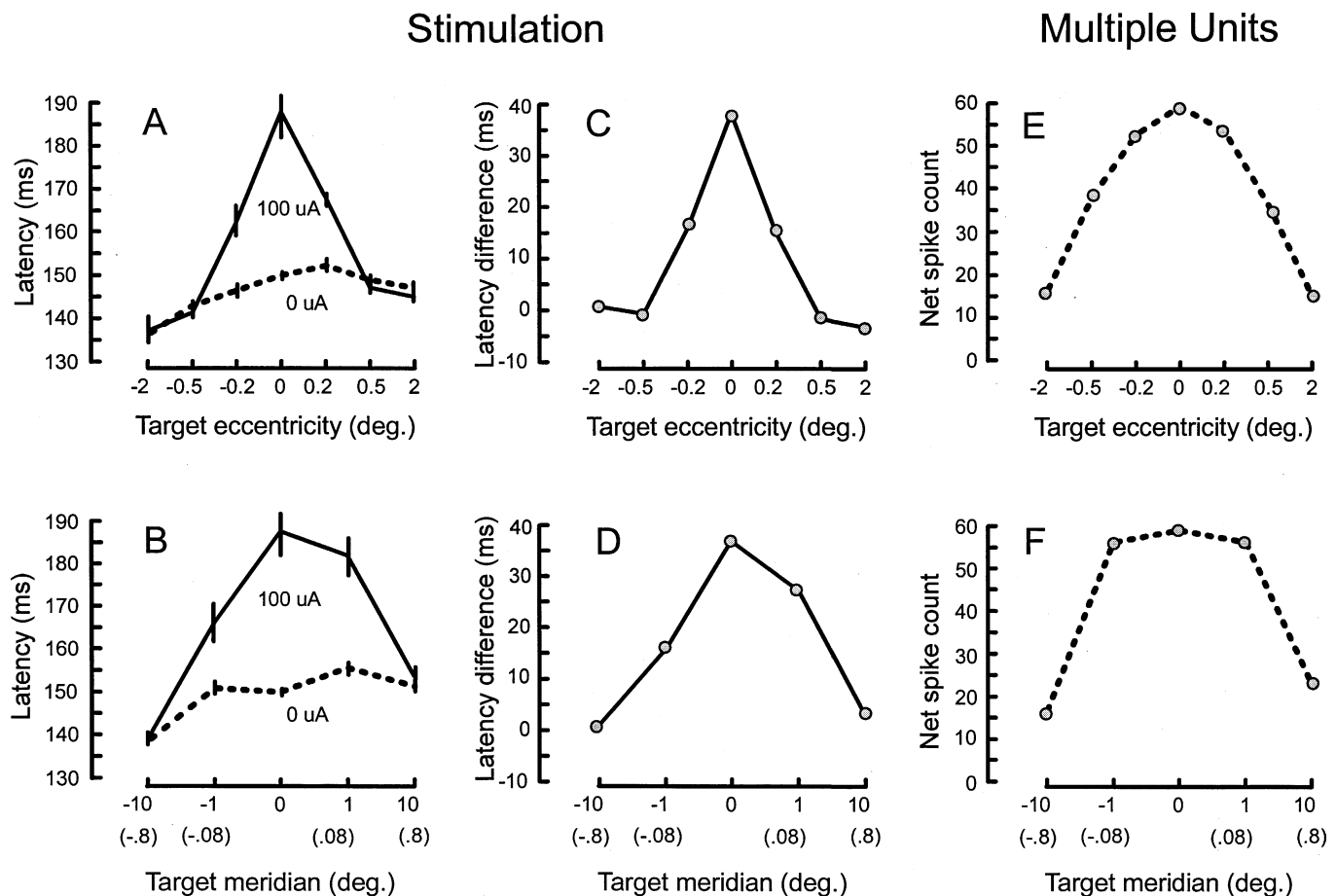


FIG. 2. Effect of stimulation on saccadic latency for different target positions at and outside of the receptive field of the stimulated neurons. (A) The latency of visually guided saccades to the target is plotted as a function of target eccentricity with respect to the receptive field of the stimulated neurons. A zero eccentricity along the x-axis indicates that the target and the receptive-field center of the stimulated neurons were in register (see Fig. 1C). Negative values along the x-axis indicate target positions situated between the fixation position and receptive-field center of the stimulated neurons. Positive values indicate target positions eccentric to the receptive-field center of the stimulated neurons. The solid curve represents data from stimulation trials and the dashed curve represents data from non-stimulation trials. Each value is based on 20 trials. Standard errors are shown. The depth of stimulation was 1.6 mm below the cortical surface. The stimulation comprised 100- $\mu$ A anode-first pulses (at 0.2-ms duration) delivered at 200 Hz using a 100-ms train. The receptive field of the stimulated units was at 233° of meridian and at 4.3° of eccentricity. The target used was brighter than background at 33% contrast and was 0.2° in diameter. Data from monkey C. For other details see Materials and methods and Fig. 1B and C. (B) The latency of visually guided saccades to the target is plotted as a function of target meridian with respect to the receptive field of the stimulated neurons. A zero meridian value along the x-axis indicates that the target and the receptive-field center of the stimulated neurons were in register (see Fig. 1C). Negative values along the x-axis indicate that the target positions had low meridian values, and positive values indicate that the target positions had high meridian values. The meridian values in parentheses are in degrees of visual angle. The solid curve represents data from stimulation trials and the dashed curve represents data from non-stimulation trials. Each value is based on 20 trials. Standard errors are shown. For other details see A. (C) The latency difference between stimulation and non-stimulation trials for the generation of visually guided saccades to the target is plotted as a function of target eccentricity with respect to the receptive-field location of the stimulated neurons for a 100- $\mu$ A current (data derived from A). See A for other details. (D) The latency difference between stimulation and non-stimulation trials for the generation of visually guided saccades to the target is plotted as a function of target meridian with respect to the receptive-field location of the stimulated neurons for a 100- $\mu$ A current (data derived from B). The meridian values in parentheses are in degrees of visual angle. See B for other details. (E) Net spike count for multiple units is plotted as a function of the target eccentricity at which the target used in the stimulation experiments (A and C) was flashed for 100 ms about the receptive field of neurons at the site of stimulation in A and C. The net spike count was determined by subtracting the spike rate of the control trials from the spike rate of the target trials. Each value is based on 20 trials. The target used was brighter than background at 33% contrast and was 0.2° in diameter. For other details see A and C, Materials and methods and Fig. 1B and C. (F) Net spike count for multiple units is plotted as a function of the target meridian at which the target used in the stimulation experiments (B and D) was flashed for 100 ms about the receptive field of neurons at the site of stimulation in B and D. The meridian values in parentheses are in degrees of visual angle. The net spike count was determined by subtracting the spike rate of the control trials from the spike rate of the target trials. Each value is based on 20 trials. The target used was brighter than background at 33% contrast and was 0.2° in diameter. For other details see B and D, Materials and methods and Fig. 1B and C.

was determined by measuring the delay effect for different target locations with respect to the center of the receptive field, i.e. along the axis of eccentricity and along the arc of meridian which pass through the receptive field center (see Fig. 1C). All values in the abscissae of Fig. 5 are expressed in degrees of visual angle. The size of the delay field measured along the axis of eccentricity and along the arc of meridian were 0.21 and 0.21 mm, respectively, for

the first site (Fig. 5A) and 0.21 and 0.20°, respectively, for the second site (Fig. 5B). The correspondence between eccentricity and meridian measures suggests that the delay field is roughly circular, although off-axis elongation is not precluded. Similar results were found for the shape of the receptive field of the neurons at the site of stimulation (Fig. 5A, 1.2 by 0.9° unit field; Fig. 5B, 0.9 by 0.8° unit field).

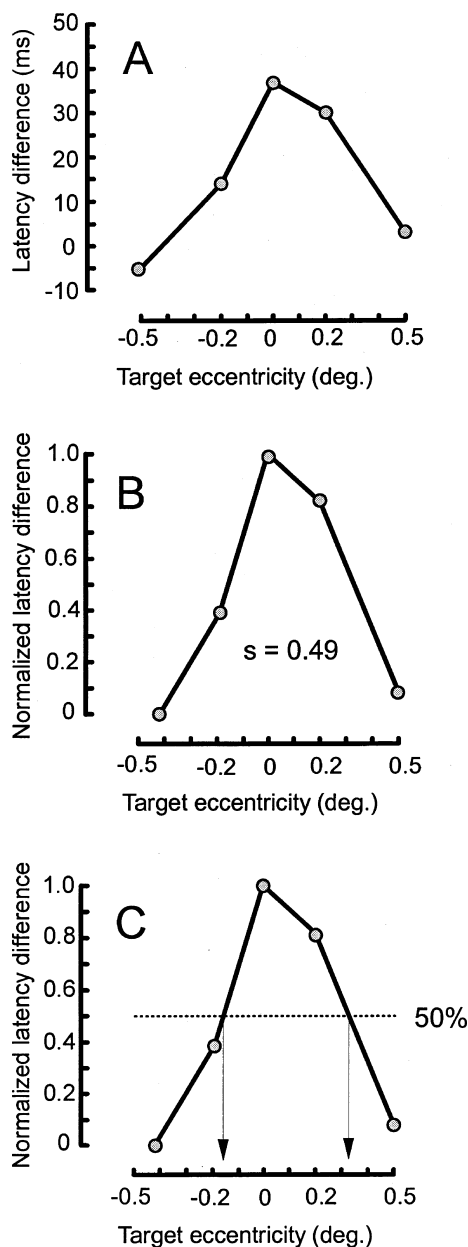


FIG. 3. Measuring the size of a delay field. The latency difference between stimulation and non-stimulation trials for the generation of visually guided saccades to the target is plotted as a function of target eccentricity with respect to the receptive field of the stimulated neurons for a V1 site whose receptive-field center was  $4.3^\circ$  from the fovea. Stimulation comprised  $100\text{-}\mu\text{A}$  anode-first pulses (at  $0.2\text{-ms}$  duration) delivered at  $200\text{ Hz}$  using a  $100\text{-ms}$  train. The target used was brighter than background at  $33\%$  contrast and was  $0.2^\circ$  in diameter. Data from monkey C. For other details see Fig. 2A and C, Materials and methods and Fig. 1B and C. (B) The latency data from above were normalized such that the values spanned the range from zero to one. (C) The size of a delay field was measured by noting the negative and positive target-eccentricity values at  $50\%$  of maximal latency difference [ $\text{size} = (0.33 - (-0.16))^\circ$ ]. The size of the delay field ( $s$ ) derived from the data in A is  $0.49^\circ$  of visual angle. This is indicated in B.

#### Size of the delay field vs. the size of the multiple-unit field

Here we address the question of what the relationship is between the size of the multiple-unit receptive field of V1 neurons and the delay field produced by electrically stimulating these neurons. At

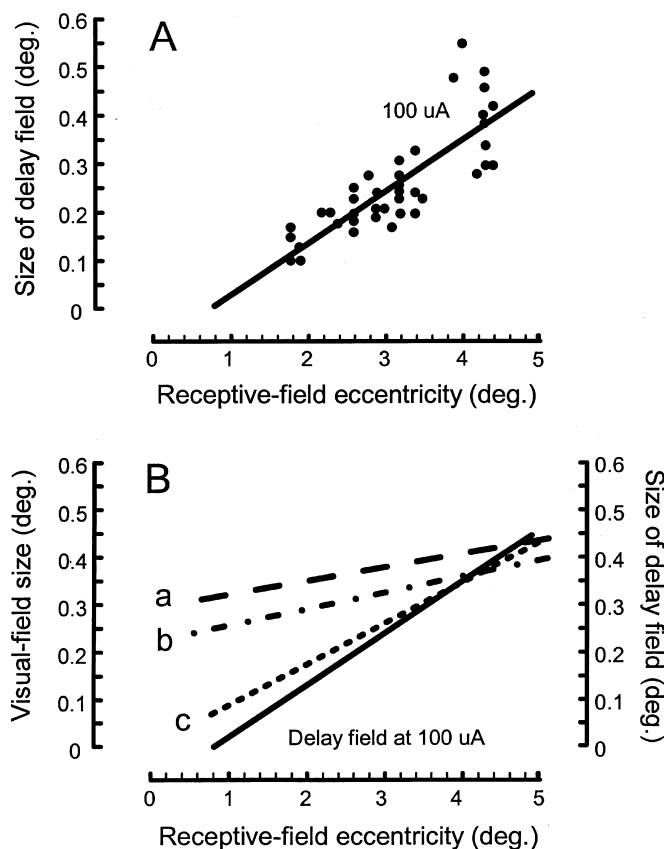


FIG. 4. Size of the delay field varies with the site of stimulation within the operculum of V1. (A) Size of the delay field is plotted as a function of the eccentricity of the receptive-field center of the V1 cells stimulated. The size of a field was determined using the method of Fig. 3C. A total of 41 V1 sites were studied using monkeys C, H and M. Sites were located from  $0.9$  to  $2.0\text{ mm}$  below the cortical surface. At each site, stimulation comprised  $100\text{-}\mu\text{A}$  anode-first pulses (at  $0.2\text{-ms}$  duration) delivered at  $200\text{ Hz}$  using a  $100\text{-ms}$  train. The target used was brighter than background at  $33\%$  contrast and was  $0.2^\circ$  in diameter. The solid curve is a regression line representing the data ( $r = 0.81$ ,  $n = 41$ ,  $P < 0.01$ ). For other details see Figs 1 and 2 and Materials and methods. (B) The relationship between average receptive-field size (in visual field coordinates) for macaque V1 and receptive-field eccentricity [(a) Hubel & Wiesel, 1974; (b) Dow *et al.*, 1981] and the relationship between amount of visual field represented by activation of a  $0.75\text{-mm}$ -diameter region of macaque V1 and receptive-field eccentricity using the complex logarithmic function of Schwartz (1994) (c) are compared to the relationship between the size of the delay field and receptive-field eccentricity using a  $100\text{-}\mu\text{A}$  current (from A).

stimulation currents of  $100\text{ }\mu\text{A}$  the delay field was consistently smaller than the receptive field of multiple units. This is shown in Figs 5 and 6. In Fig. 5, the delay field was roughly one-fifth the size of the receptive field of the neurons at the site of stimulation for the two cases (Fig. 5A,  $0.21$  by  $0.21^\circ$  delay field vs. a  $1.2$  by  $0.9^\circ$  unit field; Fig. 5B,  $0.21$  by  $0.20^\circ$  delay field vs. a  $0.9$  by  $0.8^\circ$  unit field). Figure 6 compares the size of the delay field with the size of the multiple-unit field for ten V1 sites whose units had receptive-field centers from  $4.0$  to  $4.4^\circ$  from the fovea. In all cases the delay field was smaller than the multiple-unit field (average delay field,  $0.39^\circ$  in visual angle; average unit field,  $1.65^\circ$  in visual angle;  $t_9 = 5.7$ ,  $P < 0.01$ ).

For all 41 sites tested within the operculum of V1 and tested with currents of  $100\text{ }\mu\text{A}$ , the size of the delay field was always less than the size of the multiple-unit field ( $t_{40} = 9.7$ ,  $P < 0.01$ ). For 34 sites studied, the multiple units responded to a visual stimulus (i.e.  $0.2^\circ$  in diameter at  $33\%$  contrast) presented out to  $2^\circ$  from the center of the

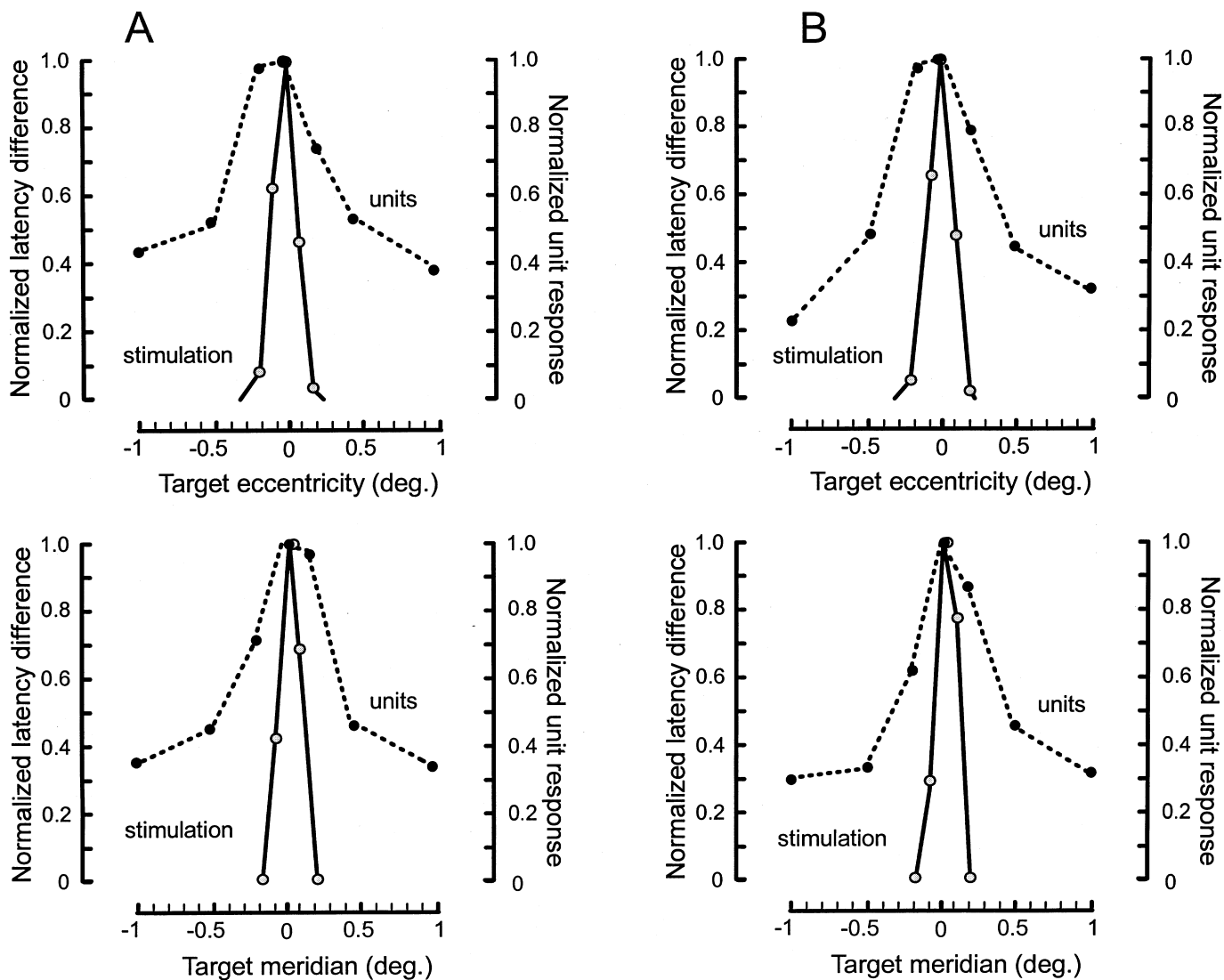


FIG. 5. Shape of the delay field as compared with the shape of the receptive field of the multiple units at the site of stimulation. (A) Normalized latency difference is plotted as a function of target eccentricity (top panel) and target meridian (bottom panel) for stimulation of one V1 site (solid curves). In addition, the normalized multiple unit response at the stimulation site to a flashed visual target is plotted as a function of target eccentricity and target meridian (dashed curves). The spike-count data were normalized to occupy a range from zero to one. Note that for the target eccentricities tested the unit response never fell to zero. All eccentricity and meridian values are plotted in degrees of visual field angle. The stimulation site was located 1.5 mm below the cortical surface and the receptive-field center of the units at the site was located at  $212^\circ$  of meridian and at  $3.2^\circ$  of eccentricity. The size of the delay field using a 50% maximal response criterion based on eccentricity (top panel) and meridian values (bottom panel) is  $0.21$  and  $0.21^\circ$ , respectively (see Fig. 3C for details). Using the same criterion, the size of the multiple-unit field for eccentricity and meridian is  $1.2$  and  $0.9^\circ$ , respectively. Stimulation comprised  $100\text{-}\mu\text{A}$  anode-first pulses (at  $0.2\text{-ms}$  duration) delivered at  $200\text{ Hz}$  using a  $100\text{-ms}$  train. The target used was brighter than background at  $33\%$  contrast and was  $0.2^\circ$  in diameter. Data from monkey C. For other details see Figs 1 and 2 and Materials and methods. (B) Normalized latency difference is plotted as a function of target eccentricity (top panel) and target meridian (bottom panel) for stimulation of one V1 site (solid curves). Also, the normalized multiple-unit response at the stimulation site to a flashed visual target is plotted as a function of target eccentricity and target meridian (dashed curves). The stimulation site was located  $1.75\text{ mm}$  below the cortical surface and the receptive-field center of the units at the site was located at  $212^\circ$  of meridian and at  $3.2^\circ$  of eccentricity. The size of the delay field using a 50% maximal response criterion based on eccentricity (top panel) and meridian values (bottom panel) is  $0.21$  and  $0.20^\circ$ , respectively (see Fig. 3C for details). Using the same criterion, the size of the multiple-unit field for eccentricity and meridian is  $0.9$  and  $0.8^\circ$ , respectively. See A for all other details.

receptive field (the greatest distance tested). These sites contained cells with receptive-field centers ranging from  $1.8$  to  $4.4^\circ$  of eccentricity. The size of the multiple-unit field increased with the eccentricity coded by the units at the site of study in the operculum ( $r = 0.33$ ,  $n = 41$ ,  $P < 0.05$ ).

#### Current spread estimates for the direct excitation of neurons

Current delivered to neural tissue through a microelectrode spreads effectively proportional to the square root of the current divided by a

current–distance constant (Tehovnik, 1996). For large pyramidal tract cells, this constant can range from  $300$  to  $3000\ \mu\text{A}/\text{mm}^2$  with an average of about  $1000\ \mu\text{A}/\text{mm}^2$  (Stoney *et al.*, 1968). These values were computed using a cathode current pulse having a duration of  $0.2\text{ ms}$ . The current–distance constant reflects the excitability of a neural element  $1\text{ mm}$  away from the electrode tip: an element having a constant of  $1000\ \mu\text{A}/\text{mm}^2$  would require a  $1000\text{-}\mu\text{A}$  current to be activated  $1\text{ mm}$  away 50% of the time. The greater the current–distance constant the less the conduction velocity of an axonal element (Jankowska & Roberts, 1972; Roberts & Smith, 1973; Hentall *et al.*,

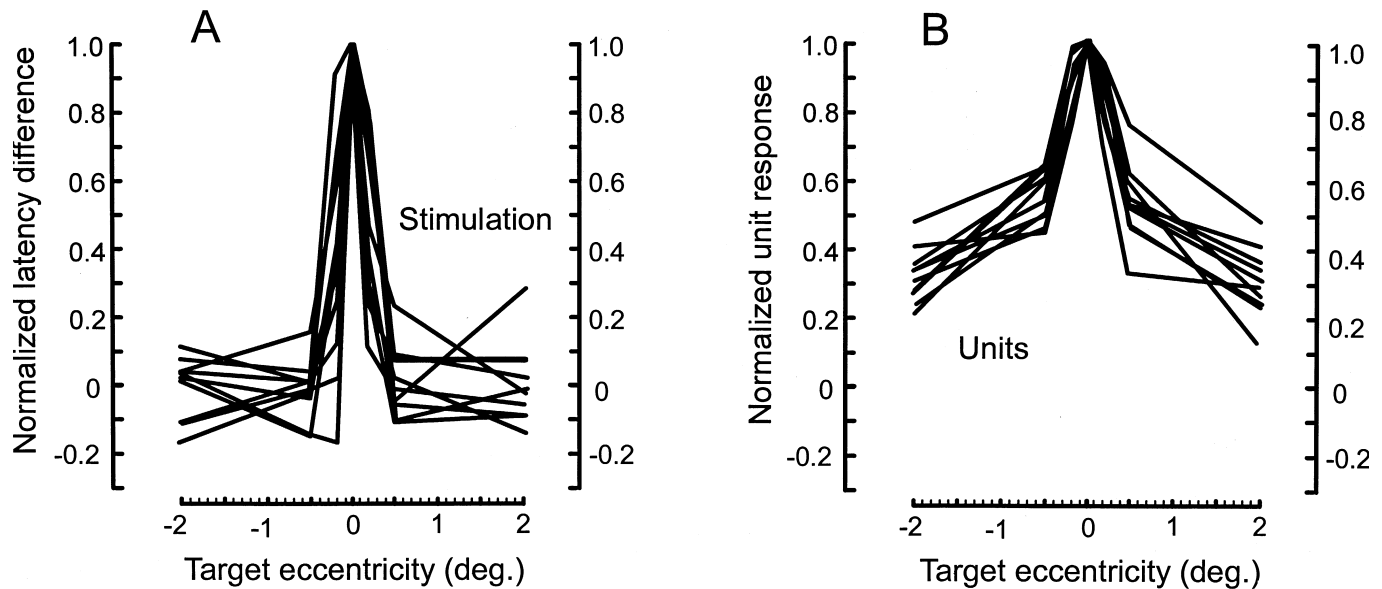


FIG. 6. Size of the delay field as compared with the size of the receptive field of the multiple units at the site of stimulation. (A) Normalized latency difference is plotted as a function of target eccentricity for ten stimulation sites (solid black curves). The latency data were normalized using the method of Fig. 3C. Stimulation comprised 100- $\mu$ A anode-first pulses (at 0.2-ms duration) delivered at 200 Hz using a 100-ms train. The target used was brighter than background at 33% contrast and was 0.2° in diameter. (B) Normalized unit response is plotted as a function of target eccentricity for the neurons at the ten stimulation sites (solid black curves). The spike-count data were normalized to range from zero to one. Note that for the target eccentricities tested the unit response never fell to zero. The receptive-field centers of the stimulation sites ranged from 4 to 4.4° from the fovea. Data from monkeys C and D. See A and Figs 1–3 for other details.

1984). Therefore, the size of a neuron's axon, and whether or not it is myelinated, are related to the current–distance constant.

To estimate the spread of current in V1, we assume a current–distance constant of 1000  $\mu$ A/mm<sup>2</sup>. This is a conservative estimate for V1 given that the neuronal elements in V1 of primates tend to be smaller and therefore less excitable than those of other parts of cerebral cortex (Cragg, 1967; Rockel *et al.*, 1980; O'Kusky & Colonnier, 1982; Fries, 1984; Peters, 1987). Indeed, the conduction velocities of pyramidal neurons exiting V1 tend to be significantly lower than those of large pyramidal neurons (Finlay *et al.*, 1976; Macpherson *et al.*, 1982). Using the equation,  $r = (I/K)$ , where  $r$  is the radius of effective current spread from the electrode tip (mm),  $I$  is the current used ( $\mu$ A) and  $K$  is the current–distance constant ( $\mu$ A/mm<sup>2</sup>), a 50–100- $\mu$ A current delivered to V1 is estimated to activate elements directly within 224–316  $\mu$ m, respectively, from the electrode tip.

## Discussion

When electrical stimulation was delivered to V1 during active fixation, the execution of a saccadic eye movement made to a visual target positioned in the receptive field of the stimulated neurons was delayed. No delay was obtained when the visual target was placed at locations outside of the receptive field. The magnitude of the delay effect was greatest when the visual target was positioned in the center of the receptive field of the stimulated neurons. The delay effect decreased as the visual target was placed at progressively greater distances from the center of the visual receptive field of the stimulated neurons. These findings are consistent with previous reports (Tehovnik *et al.*, 2004; Tehovnik & Slocum, 2005).

The size of the delay field induced by electrical stimulation was smallest for those neurons that had their receptive fields near the fovea and became progressively larger with increasing eccentricity. Stimulation sites at which neurons had receptive fields 2° from the center of gaze had delay fields measuring (on average) 0.14° in

diameter when current levels of 100  $\mu$ A were used; stimulation sites at which neurons had their receptive fields 4° from the fovea had delay fields measuring 0.35° using a similar current level (Fig. 4A). When the current was reduced to 50  $\mu$ A, the size of the delay field was reduced by 26%. Delay fields were circular rather than elongated, much like visual receptive fields as determined by recording multiple-unit activity at the site of stimulation and much like phosphenes induced by electrical stimulation of human V1 (Brindley & Lewin, 1968; Dobbelle & Mladejovsky, 1974; Schmidt *et al.*, 1996).

### Volume of tissue activated to evoke the saccadic delay

How far current spreads effectively in V1 tissue can be estimated by noting the size of visual field affected by a current (Tehovnik *et al.*, 2004). The following example is based on delay-field data collected for an eccentricity of 3° (Fig. 4A). Here the size of visual field affected by a 100- $\mu$ A current was 0.24° (on average). At a 3° eccentricity, 1000  $\mu$ m of V1 tissue represents about 0.32° of visual field, which is based on the cortical magnification factor of macaque V1 (Hubel & Wiesel, 1974; Dow *et al.*, 1981; Tootell *et al.*, 1988). Therefore, 100  $\mu$ A affects V1 tissue within 375  $\mu$ m from the electrode tip (i.e. 0.24°/0.32°  $\times$  1000  $\mu$ m/2). This estimate is similar to, although somewhat greater than, that calculated with the current–distance equation for the direct activation of V1 elements with a 0.2-ms electrical pulse [100- $\mu$ A currents affect V1 tissue within 316  $\mu$ m from the electrode tip (see Results)]. Therefore, much of the delay effect is apparently due to the direct activation of V1 elements.

### Spread of the unit signal while recording with low-impedance electrodes

The present study shows that when recording from multiple units in the operculum of V1 using low-impedance electrodes (ranging from 0.3 to

0.5 M $\Omega$  tested at 1 kHz) the cells discharge to a punctate visual stimulus (0.2°) presented out to 2° from the center of the receptive field. The visual-field distance of 2° for neurons coding for 3° of eccentricity, for example, translates into a cortical distance of roughly 6 mm from the electrode tip (using the calculation from the preceding section). There are two possible explanations for this broad recording field. First, the low-impedance electrodes used by us may be sampling activity well beyond that normally observed with high-impedance electrodes (impedance > 1.0 M $\Omega$ ). Second, activation of single cells in V1 might excite the lateral connections within V1 (Fisken *et al.*, 1973; McGuire *et al.*, 1991), thereby increasing the size of the recording field.

### *Making inferences about phosphenes by stimulation of macaque V1*

In humans, stimulating electrodes placed at progressively more distant locations from the foveal representation of V1 produce increasingly larger phosphenes (Brindley & Lewin, 1968). Phosphenes in most cases have a circular configuration with sizes under 3° even for stimulation sites most extreme from the foveal representation (Brindley & Lewin, 1968; Dobbelle & Mladejovsky, 1974; Schmidt *et al.*, 1996). These findings correspond well with the receptive field properties of V1 cells as described for macaque monkeys (Hubel & Wiesel, 1974; Schiller *et al.*, 1976; Dow *et al.*, 1981; Van Essen *et al.*, 1984).

That electrical stimulation of V1 in monkeys induces a phosphene was first suggested by the work of Doty and colleagues (Doty, 1965, 1970; Bartlett & Doty, 1980; Bartlett *et al.*, 2005; DeYoe *et al.*, 2005). Monkeys were trained to depress a lever for reward after the delivery of electrical stimulation to V1. It was presumed in these experiments that during stimulation of V1 monkeys experience a unitary and punctate visual percept because the conditioning effect attributed to stimulation of V1 was immediately generalized to any ipsilateral or contralateral location within the V1 map (Doty, 1965, 1970) and because the conditioning response was obtained using currents as low as 1–2  $\mu$ A (Bartlett & Doty, 1980; DeYoe *et al.*, 2005). Furthermore, the excitability properties of V1 elements mediating the conditioned response were restricted, suggesting that a limited population of neurons mediates this response (Bartlett *et al.*, 2005). Finally, the excitability of these neuronal elements was similar to the excitability of those that mediate stimulation-elicited phosphenes from human V1 (Brindley & Lewin, 1968; Dobbelle & Mladejovsky, 1974; Rushton & Brindley, 1978). Therefore, every time stimulation elicits a conditioning response by excitation of monkey V1, a phosphene is probably experienced by the animal.

Additional evidence for the idea that monkeys experience a phosphene during electrical stimulation of V1 comes from the work of Troyk, Bradley and colleagues (Troyk *et al.*, 2003; Bradley *et al.*, 2005). They trained a monkey to generate memory-guided saccadic eye movements to the receptive-field location of V1 neurons stimulated electrically. This procedure divorces the effect of stimulation from the motor response; therefore, it was presumed that the monkey was generating a saccade toward a remembered phosphene.

Based on the foregoing, we believe that the size of a delay field can be used as an estimate of the phosphene size as evoked electrically from macaque V1. Two observations support this inference. First, as mentioned earlier, the V1 elements that mediate the saccadic delay exhibit excitability properties similar to those reported for neurons activated in human V1 to produce a phosphene (Tehovnik *et al.*, 2004). Second, as with phosphenes induced in humans, the size of a delay field increases as the stimulating electrode is positioned at a greater distance from the foveal representation in V1 (current study).

In a previous publication, we have suggested that the size of a phosphene produced in V1 is dependent on the receptive-field size of the directly stimulated neurons (Tehovnik *et al.*, 2005). Because the average receptive field size of single units increases with increasing distance from the foveal representation of V1 (Hubel & Wiesel, 1974; Dow *et al.*, 1981), one might expect the size of an evoked phosphene to increase with eccentricity, as has been found in humans by Brindley & Lewin (1968). On initial inspection this seems to be true, but the slope of the function for the size of delay fields across eccentricity differs from that of the function for the size of receptive fields (Fig. 4B, a and b). In addition, at the lowest eccentricities (e.g. 2°), the size of the delay fields are less than the size of receptive fields.

The center of a visual receptive field of V1 cells provides a point-to-point mapping between visual and cortical space, based on the cortical magnification factor (Hubel & Wiesel, 1974; Dow *et al.*, 1981; Tootell *et al.*, 1988). One can map the region of current spread (in cortex) to a corresponding region in visual space (the putative phosphene). If one assumes that the distance that current spreads effectively in V1 is invariant for a given current, regardless of the location of stimulation, then phosphene size should increase with eccentricity according to the cortical magnification factor.

To predict phosphene size precisely using the cortical magnification factor, the complex logarithmic function of Schwartz (1994) can be used. Using this model, with a realistic model parameter for macaque ( $a = 0.3$ ; Schwartz, 1994), it is possible to calculate the size of the inferred phosphene as a function of eccentricity for a given size of current spread. For current equal to 100  $\mu$ A (corresponding to activation of V1 tissue in a region with diameter 0.75 mm, as estimated earlier), anticipated phosphene size as calculated using the Schwartz model is shown (Fig. 4B, c). Note the substantial agreement between the model and our experimental result for delay field size (Fig. 4B; the slopes of the two functions are similar). Thus, the size of a delay field coincides with phosphene size when derived from the cortical magnification factor.

Future studies will be needed to determine how cortical magnification factor and receptive field size co-vary with the spatial properties of a delay field, especially for V1 sites beyond the operculum that code for extreme visual field eccentricities. How cortical magnification factor and receptive field size contribute to phosphene induction deserves serious study using a variety of behavioral methods, one of which is described in this report. Determining more thoroughly what a monkey sees when microstimulation is delivered to V1 should accelerate the development of an effective V1 prosthesis for the blind.

### Acknowledgements

We thank Ms Christina Carvey in helping in the preparation of the manuscript. NIH EY014884 to P.H.S. supported this work.

### Abbreviation

V1, primary visual cortex.

### References

- Bartlett, J.R., DeYoe, E.A., Doty, R.W., Lee, B.B., Lewine, J.D., Negrão, N. & Overman, W.H. (2005) Psychophysics of electrical stimulation of striate cortex in macaques. *J. Neurophysiol.*, **94**, 3430–3442.
- Bartlett, J.R. & Doty, R.W. (1980) An exploration of the ability of macaques to detect microstimulation of striate cortex. *Acta Neurobiol. Exp. (Warsz.)*, **40**, 713–728.

- Bradley, D.C., Toyk, P.R., Berg, J.A., Cogan, M., Erickson, R., Kufta, C., Mascaro, M., McCreery, D., Schmidt, E.M., Towle, V.L. & Xu, H. (2005) Visuotopic mapping through multichannel stimulating implant in primate V1. *J. Neurophysiol.*, **93**, 1659–1670.
- Brindley, G.S. & Lewin, W.S. (1968) The sensations produced by electrical stimulation of visual cortex. *J. Physiol. (Lond.)*, **196**, 479–493.
- Cragg, B.G. (1967) The density of synapses and neurons in the motor and visual areas of the cerebral cortex. *J. Anat.*, **101**, 639–654.
- DeYoe, E.A., Lewine, J. & Doty, R.W. (2005) Laminar variation in threshold for detection of electrical excitation of striate cortex in macaques. *J. Neurophysiol.*, **94**, 3443–3450.
- Dobelle, W.H. & Mladejovsky, M.G. (1974) Phosphenes produced by electrical stimulation of human occipital cortex, and their application to the development of a prosthesis for the blind. *J. Physiol. (Lond.)*, **243**, 553–576.
- Doty, R.W. (1965) Conditioned reflexes elicited by electrical stimulation of the brain in macaques. *J. Neurophysiol.*, **28**, 623–640.
- Doty, R.W. (1970) On butterflies in the brain. In: Rusinov, W.S. (Ed.), *Electrophysiology of the Central Nervous System*. Plenum Press, New York, pp. 97–106.
- Dow, B.M., Snyder, A.Z., Vautin, R.G. & Bauer, R. (1981) Magnification factor and receptive field size in foveal striate cortex of the monkey. *Exp. Brain Res.*, **44**, 213–228.
- Finlay, B.L., Schiller, P.H. & Volman, S.F. (1976) Quantitative studies of single-cell properties in monkey striate cortex. IV. Corticotectal cells. *J. Neurophysiol.*, **39**, 1352–1361.
- Fisken, R.A., Garey, L.J. & Powell, T.P.S. (1973) Patterns of degeneration after intrinsic lesions of the visual cortex (area 17) of the monkey. *Brain Res.*, **53**, 208–213.
- Fries, W. (1984) Cortical projections to the superior colliculus in the macaque monkey: a retrograde study using horseradish peroxidase. *J. Comp. Neurol.*, **230**, 55–76.
- Hentall, I.D., Zorman, G., Kansky, S. & Fields, H.L. (1984) Relations among threshold, spike height, electrode distance, and conduction velocity in electrical stimulation of certain medullospinal neurons. *J. Neurophysiol.*, **51**, 968–977.
- Hubel, D.H. & Wiesel, T.N. (1974) Uniformity of monkey striate cortex: a parallel relationship between field size, scatter, and magnification factor. *J. Comp. Neurol.*, **158**, 295–306.
- Jankowska, E. & Roberts, W.J. (1972) An electrophysiological demonstration of the axonal projections of single spinal interneurons in the cat. *J. Physiol. (Lond.)*, **222**, 597–622.
- Judge, S.J., Richmond, B.L. & Chu, F.C. (1980) Implantation of magnetic search coils for measurement of eye position: an improved method. *Vision Res.*, **20**, 535–538.
- Kammer, T., Puls, K., Strasburger, H., Hill, N.J. & Wichmann, F.A. (2005) Transcranial magnetic stimulation in the visual system. I. The psychophysics of visual perception. *Exp. Brain Res.*, **160**, 118–128.
- Macpherson, J., Wiesendanger, M., Marangoz, C. & Miles, T.S. (1982) Corticospinal neurons of the supplementary motor area of monkeys: a single unit study. *Exp. Brain Res.*, **48**, 81–88.
- McGuire, B.A., Gilbert, C.D., Rivlin, P.K. & Wiesel, T.N. (1991) Targets of horizontal connections in macaque primary visual cortex. *J. Comp. Neurol.*, **305**, 370–392.
- O’Kusky, J. & Colonnier, M. (1982) A laminar analysis of the number of neurons, glia, and synapses in the visual cortex (area 17) of adult macaque monkeys. *J. Comp. Neurol.*, **210**, 278–290.
- Peters, A. (1987) Number of neurons and synapses in primary visual cortex. In: Jones, E.G. & Peters, A. (Eds), *Cerebral Cortex*, **Vol. 6**. Plenum Press, New York, pp. 267–294.
- Roberts, W. & Smith, D.O. (1973) Analysis of threshold currents during microstimulation of fibres in the spinal cord. *Acta Physiol. Scand.*, **89**, 384–394.
- Rockel, A.J., Hiorns, R.W. & Powell, T.P.S. (1980) The basic uniformity in structure of the neocortex. *Brain*, **103**, 221–244.
- Rushton, D.N. & Brindley, G.S. (1978) Properties of cortical electrical phosphenes. In: Cool, S.J. & Smith, E.L. (Eds), *Frontiers in Visual Science*. Springer-Verlag, New York, pp. 574–593.
- Schiller, P.H., Finlay, B.L. & Volman, S.F. (1976) Quantitative studies of single-cell properties in monkey striate cortex. I. Spatiotemporal organization of receptive fields. *J. Neurophysiol.*, **39**, 1288–1319.
- Schiller, P.H. & Tehovnik, E.J. (2001) Look and see: how the brain moves your eyes about. *Prog. Brain Res.*, **134**, 127–142.
- Schmidt, E.M., Bak, M.J., Hambrecht, F.T., Kufta, C.V., O’Rourke, D.K. & Vallabhanath, P. (1996) Feasibility of a visual prosthesis for the blind based on intracortical microstimulation of the visual cortex. *Brain*, **119**, 507–522.
- Schwartz, E.L. (1994) Computational studies of the spatial architecture of primate visual cortex: columns, maps, and protomaps. In: Peters, A. & Rockland, K.S. (Eds), *Cerebral Cortex*. Plenum Press, New York, pp. 359–411.
- Slocum, W.M. & Tehovnik, E.J. (2004) Microstimulation of V1 input layers disrupts the selection and detection of visual targets by monkeys. *Eur. J. Neurosci.*, **20**, 1674–1680.
- Stoney, S.D., Thompson, W.D. & Asanuma, H. (1968) Excitation of pyramidal tract cells by intracortical stimulation: effective extent of stimulating current. *J. Neurophysiol.*, **31**, 659–669.
- Tehovnik, E.J. (1996) Electrical stimulation of neural tissue to evoke behavioural responses. *J. Neurosci. Meth.*, **65**, 1–17.
- Tehovnik, E.J. & Slocum, W.M. (2003) Microstimulation of macaque V1 disrupts target selection: effects of stimulation polarity. *Exp. Brain Res.*, **148**, 233–237.
- Tehovnik, E.J. & Slocum, W.M. (2005) Microstimulation of V1 affects the detection of visual targets: manipulation of target contrast. *Exp. Brain Res.*, **165**, 305–314.
- Tehovnik, E.J., Slocum, W.M., Carvey, C.E. & Schiller, P.H. (2005) Phosphenes induction and the generation of saccadic eye movements by striate cortex. *J. Neurophysiol.*, **93**, 1–19.
- Tehovnik, E.J., Slocum, W.M. & Schiller, P.H. (2002) Differential effects of laminar stimulation of V1 cortex on target selection by macaque monkeys. *Eur. J. Neurosci.*, **16**, 751–760.
- Tehovnik, E.J., Slocum, W.M. & Schiller, P.H. (2003) Saccadic eye movements evoked by microstimulation of striate cortex. *Eur. J. Neurosci.*, **17**, 870–878.
- Tehovnik, E.J., Slocum, W.M. & Schiller, P.H. (2004) Microstimulation of V1 delays the execution of visually guided saccades. *Eur. J. Neurosci.*, **20**, 264–272.
- Tootell, R.B.H., Switkes, E., Silverman, M.S. & Hamilton, S.L. (1988) Functional anatomy of macaque striate cortex. II. Retinotopic organization. *J. Neurosci.*, **8**, 1531–1568.
- Troyk, P., Bak, M., Berg, J., Bradley, D., Cogan, S., Erickson, R., Kufta, C., McCreery, D., Schmidt, E. & Towle, V. (2003) A model for intracortical visual prosthesis research. *Artificial Organs*, **27**, 1005–1015.
- Van Essen, D.C., Newsome, W.T. & Maunsell, J.H.R. (1984) The visual field representation in striate cortex of the macaque monkey: asymmetries, anisotropies, and individual variability. *Vision Res.*, **24**, 429–448.